International Journal of Engineering & Technology, 7 (4.36) (2018) 103-111

International Journal of Engineering & Technology

Website: www.sciencepubco.com/index.php/IJET

Research paper

A Study on Ship Manoeuvring Simulation and Ship Trajectory Optimization Based on Sqp and Bfgs Algorithms from Sea Trials

Tran Khanh Toan

Vietnam Maritime University (VIMARU), Faculty of Civil Engineering,
No. 484 Lach Tray street, 180000, Haiphong city, Vietnam
**Corresponding author: toantk.ctt@vimaru.edu.vn, Phone (84) 915 66 96 86*

Abstract

In this study, a procedure is proposed to optimize the ship's trajectory by identification of optimal hydrodynamic coefficients from sea trials, which coupled the dynamic ship motion model with optimization techniques. In order to assess efficiently the hydrodynamic parameters, a sensitivity analysis is first per- formed to identify the most sensitive coefficients, then an identification procedure, based on SQP and BFGS algorithms, is carried out to determine optimal hydrodynamic parameters. The validation of this procedure is done for Turning Circle and Zig-Zag tests by using experimental data of sea trials of the Esso Bernicia 193000DWT Tanker model. Comparisons between experimental and computed data show a fair agreement of overall tendency in ship trajectories. The *RMSD* (Root-Mean-Square Deviation) of ship trajectory decreases from 68.0*m* to 5.8*m* in Turning Circle test, and *RMSD* of yaw angle decreases from 17.3*deg* to 6.6*deg* in Zig-Zag test.

Keywords: *Ship maneuvering, hydrodynamics, parameters identification, ship motion, mathematical programming*

1. Introduction

Ship maneuvering models are fundamental to the research of ship maneuverability, design of ship motion control systems and development of ship handling simulators. The complexity of the hydrodynamic processes caused by the wide variety of ship shapes, sizes and motion leads to a multitude of ship models. Thus, to obtain an optimized trajectory and also a better understanding of ship maneuvering it is necessary to improve the understanding of the hydrodynamic forces acting on the hull, the rudder and the propeller. Many mathematical models of dynamic ship motion have been proposed to identify the hydrodynamic parameters [1], [2] and [3]. Hyeon Kyu Yoon et al. [4] proposed a model based on the Estimation-Before-Modeling (EBM) technique, which is an identification method that estimates parameters in a dynamic model. The algorithm was validated using real sea trial data of a 113*K* tanker. Viviani et *al*. [5] carried out a numerical study based on optimization techniques that used a Multi Objective Genetic Algorithm (MOGA). They identified the five most sensitive hydrodynamic parameters from standard maneuvers (specified by International Maritime Organization - IMO) for a series of twin-screw ships. Rajesh et al. [6] Proposed a numerical study based on system identification for a nonlinear maneuvering model dedicated for large tankers by using the artificial neural network method. In this model all nonlinear terms are clubbed together to form one unknown time function per equation which are sought to be represented by the neural network coefficients. M.G. Seo and Y. Kim [9], proposed a numerical analysis of ship maneuvering performance in the presence of incident waves and resultant ship motion responses. To this end, a time domain ship motion program is developed to solve the wave body interaction problem with the ship slip speed and rotation, and it is coupled with a modular type 4DOF maneuvering problem. X.G. Zhang and Z.J.Zou [8] analyzed the data of longitudinal and transverse velocity, rudder angle etc. in the simulated zig-zag test, the hydrodynamic derivatives in the Abkowitz model for ship maneuvering motion are identified using E-Support Vector Re-gression (E-SVR). The identification results of the hydrodynamic derivatives are compared with the Planar Motion Mechanism (PMM) test results to verify the identification method. The agreement is satisfactory, which shows that the regressive Abkowitz model has a good generalization performance. This paper presents an efficient procedure to determine optimal hydrodynamic parameters by using the single-objective optimization techniques for ship maneuvering simulation from sea trials. Accurate modeling of a ship trajectory is achieved efficiently using three steps. The first step concerns the modeling of the dynamic ship motion, for this purpose, a $3-DOF$ model based on the dynamic motion of a rigid body has been developed taking into account the hydrodynamic forces acting on the ship hull. Then a sensitivity analysis is carried out to identify the most important hydrodynamic parameters that control the ship trajectory. The main advantage of applying the sensitivity analysis is to reduce the number of parameters to be estimated so that the hydrodynamic model can easily be treated by a single-objective minimization procedure with constraints or unconstraint, and multi-variables. In the present investigations, we found 14 most sensitive parameters, and the validated is done by using experimental data of sea trials of the Esso Bernicia 193000DWT Tanker for the turning circle and zig-zag tests. The last step of the proposed procedure concerns the determination of optimal hydrodynamic parameters using optimization techniques.

These steps in the process of identification are summarized in Table 1.

Table 1: Steps in the strategy of parameters identification process

Step 1	Step 2	Step 3
Computing with original coefficients (α) from ship motion equations	Filtering the most important coefficients (α_S), using the sensitivity analysis	Computing of optimal coefficients (α_{opt}), using the identification analysis

The structure of this paper is as follows. Section 2 deals with the mathematical formulation of the dynamic motion of ships. The Section 3 is devoted to the numerical resolution, where validation tests are presented in subsection 3.3 and results of the identification of hydrodynamic parameters procedure are presented in subsection 3.4. Section 4 summaries the conclusions drawn from this work

2. Mathematical formulation

2.1. Dynamic ship motion equations

In the ship maneuvering problem, 3 degrees of freedom ($3-DOF$) motions are considered in the space-fixed coordinate system, where all frames are right handed orthogonal coordinate systems whose z-axes are positive downward. For this problem, the equations of motion can be written as follows: [10; 17]:

$$\dot{v}+ur=gY^{"};\dot{v}+ur=gY^{"};\left(Lk_Z^{"}\right)^2\dot{r}=gLN^{"} \tag{1}$$

Where:

G is the gravity center of ship; u and v are the ship velocities in GX_0-axis (surge motion) and GY_0 axis (sway motion) respectively; r is the turning rate about GZ_0-axis (yaw motion); $\dot{u}$ and $\dot{v}$ are the ship axial accelerations in GX_0-axis and GY_0-axis respectively (see Fig. 1); $\dot{r}$ is the turning acceleration around GZ_0-axis; g is the gravity acceleration; L is the ship length between perpendiculars; $k_Z^{"}=\frac{1}{L}\sqrt{\frac{I_Z}{m}}$ is the non-dimensional radius of gyration, I_z is the inertial moment of ship with respect to GZ_0-axis, where T_s is the ship draft and ρ is the density of water.

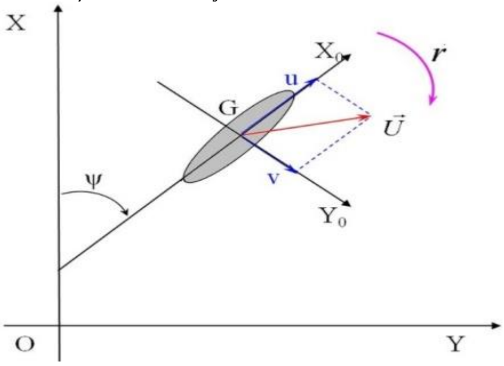

Fig.1: Definition of the ship motion coordinate system

$$\begin{aligned} g.X^{"} &= X_{\dot{u}}^{"}\dot{u}+\frac{1}{L}X_{u|u|}^{"}u|u|+\frac{1}{L}X_{vr}^{"}vr+\frac{1}{L}X_{vv}^{"}v|v| \\ &+\frac{1}{L}X_{c|c|\delta\delta}^{"}c|c|\delta^2+\frac{1}{L}X_{c|c|\beta\delta}^{"}c|c|\beta\delta+gT^{"}(1-t_d) \\ &+\frac{1}{L}X_{\dot{u}\xi}^{"}\dot{u}\xi+\frac{1}{L}X_{|u|u\xi}^{"}|u|u\xi+\frac{1}{L}X_{vr\xi}^{"}vr\xi+\frac{1}{L}X_{vv\xi\xi}^{"}v^2\xi^2 \end{aligned} \tag{2}$$

$$\begin{aligned} g.Y^{"} &= Y_{\dot{v}}^{"}\dot{v}+\frac{1}{L}Y_{uv}^{"}uv+\frac{1}{L}Y_{|v|v}^{"}|v|v+\frac{1}{L}Y_{|c|c\delta}^{"}|c|c\delta+\frac{1}{L}Y_{ur}^{"}ur \\ &+\frac{1}{L}Y_{|c|c|\beta|\beta\delta}^{"}|c|c|\beta|\beta\delta+Y_T^{"}gT+\frac{1}{L}Y_{ur\xi}^{"}ur\xi+\frac{1}{L}Y_{uv\xi}^{"}uv\xi \\ &+Y_{\dot{v}\xi}^{"}\dot{u}\xi+\frac{1}{L}Y_{|v|v\xi}^{"}|v|v\xi+\frac{1}{L}Y_{|c|c|\beta|\beta\delta\xi}^{"}|c|c|\beta|\beta\delta\xi \end{aligned} \tag{3}$$

$$\begin{aligned} g.L.N^{"} &= \frac{1}{L^2}N_{\dot{r}}^{"}\dot{r}+\frac{1}{L^2}N_{uv}^{"}uv+\frac{1}{L}N_{|v|r}^{"}|v|r \\ &+\frac{1}{L^2}N_{|c|c\delta}^{"}|c|c\delta+\frac{1}{L}N_{ur}^{"}ur+\frac{1}{L^2}N_{|c|c|\beta|\beta\delta}^{"}|c|c|\beta|\beta\delta \\ &+\frac{1}{L}N_T^{"}gT+\frac{1}{L}N_{ur\xi}^{"}ur\xi+N_{\dot{r}\xi}^{"}\dot{r}\xi+\frac{1}{L^2}N_{uv\xi}^{"}uv\xi \\ &+\frac{1}{L}N_{vr\xi}^{"}rv\xi+\frac{1}{L^2}N_{|c|c|\beta|\beta|\delta|\xi}^{"}|c|c|\beta|\beta|\delta|\xi \end{aligned} \tag{4}$$

Where:

X", *Y*", *N*" are the non-dimensional forces and moments in GX_0-axis, GY_0-axis and GZ_0-axis respectively; $X_{\dot{u}}^{"}, X_{u|u|}^{"},..., Y_{\dot{v}}^{"}, Y_{uv}^{"},..., N_{\dot{r}}^{"}, N_{uv}^{"},..., N_{|c|c|\beta|\beta|\delta|\xi}^{"}$ are the non-dimensional derivatives of ship hydrodynamic coefficients, which will be identified by SQP and BFGS algorithms; δ is the rudder angle; t_d is the thrust deduction coefficient; $\beta = v/u$.

$\xi = T_s/(h - T_s)$, where h is the water depth;

T" is the non-dimensional propeller thrust given by:

$$T^{"}=\frac{1}{gL}T_{uu}^{"}u^2+\frac{1}{g}T_{un}^{"}un+\frac{L}{g}T_{|n|n}^{"}|n|n \tag{5}$$

Where: T_{uu}, T_{un} and $T_{|n|n}$ are the hydrodynamic coefficients, n is the shaft velocity; c is the flow velocity at the rudder estimated by:

$$c^2=c_{un}^2un+c_{nn}^2n^2 \tag{6}$$

Where: c_{un} and c_{nn} are the hydrodynamic coefficients.

3. Numerical resolution

3.1. Simulation and optimization procedure

Given motion variables and the hydrodynamic forces and moment, computed at the first step from dynamic ship motion, we carried out the sensitivity analysis as the second step, and the minimization analysis to identify the hydrodynamic coefficients from hydrodynamic force as the third step. Firstly, we computed the motion variables (state of ship motions) x = $[u\ v\ r\ X_{pos}\ Y_{pos}\ \psi\ \delta\ n]^T$ as a nonlinear time-varying system:

$$\dot{x}=f(x,u_c,t) \tag{7}$$

Where: t is the time; X_{pos} and Y_{pos} are the coordinates of ship in OX-axis and OY-axis of the earth-frame respectively; $u_c = [\delta_c\ n_c]^T$ is the control input; δ_c is the commanded rudder angle; n_c is the commanded shaft velocity; $\dot{\mathbf{x}} = [\dot{u}\ \dot{v}\ \dot{r}\ \dot{X}_{pos}\ \dot{Y}_{pos}\ \dot{\psi}\ \dot{\delta}\ \dot{n}]^T$ is the vector derivative of x, which is computed simultaneously by solving the equations (1) and (8-12) by the Runge-Kutta 4th order method (RKF45) as follows:

• First, the derivatives $\dot{u}$, $\dot{v}$ and $\dot{r}$ are computed by solving equations (1)

• Then, the others derivatives $\dot{X}_{pos}, \dot{Y}_{pos}, \dot{\psi}, \dot{\delta}$ and $\dot{n}$ are computed by solving the equations (8-12) [10]:

$$\dot{X}_{pos} = \cos(\psi)u - \sin(\psi)v \tag{8}$$

$$\dot{X}_{pos} = \cos(\psi)u - \sin(\psi)v \tag{9}$$

$$\dot{\psi} = r \tag{10}$$

$$\dot{\delta} = \delta_c - \delta \tag{11}$$

$$\dot{n} = \frac{60}{T_m}(n_c - n) \tag{12}$$

where T_m is a coefficient of propeller.

In this work, a single objective function for minimization procedure with inequality constraints or unconstraint, and multi-variable is used to identify ship hydrodynamic coefficients [11]. As the sign of the hydrodynamic parameters must fit hydrodynamic forces, some constraints can be included into the minimization problem, which leads to a constrained minimization problem.

Thus, the problem is stated as follows

$$\text{Minimize } F_{obj} = \left(\sum_{i=1}^{N} f_i(\alpha)^2 \right)^{1/2} \tag{13}$$

with $\alpha = [\alpha_1, \alpha_2, ..., \alpha_N]^T$

Where:

α is the vector of identification variables which represents the ship hydrodynamic parameters to be determined; N is the number of variables; $f_i(\alpha)$ is the discrepancy between computed and experimental data.

Problem given in (13) can be solved using different approaches. One of the most efficient approach is based on the optimization techniques, where not only information on the objective-function F_{obj} are necessary but also values of the gradients of F_{obj} with respect to the vector α, are required to update the solution from one iteration to the other. Among all optimization techniques, the Sequential Quadratic Programming (SQP) algorithm [12] is a widely applicable optimization method which converges for many problems with constraint in engineering science. The BFGS (Broyden-Fletcher-Goldfarb-Shanno) algorithm [13] is a part of the family of quasi-Newton algorithms, which may be used for the unconstrained optimization problems.

In the present numerical investigations, two tests proposed by the International Maritime Organization (IMO [14]) are used, which consist of Turning Circle and Zig-Zag tests [15]. The associated input data of each test are presented in Table 2[16].

(i) For the Turning Circle test, the expression of $F_{ob\,j}$, reads:

$$F_{cbj} = \left(\sum_{i=1}^{N_p} f_i(\alpha)^2 \right)^{1/2} = \left(\sum_{i=1}^{N_p} \Delta S_i^2 \right)^{1/2} \tag{14}$$

Where: ΔS_i^2 is the square root of the difference between the computed and the experimental ship trajectories, which depends on ship hydrodynamic coefficients α. It reads:

$$\Delta S_i^2 = \left(x_i^{cal} - x_i^{\exp} \right)^2 + \left(y_i^{cal} - y_i^{\exp} \right)^2 \tag{15}$$

Table 2: Input data of Turning Circle and Zig-Zag tests of Esso Bernicia 193,000DWT Tanker [16]

Input data	Turning Circle test	Zig-Zag
(x_0, y_0): initial ship's position	(0,0) m	(0,0) m
ψ_0: initial yaw angle	0 deg	0 deg
U_0: initial advance velocity of ship	5.3 m/s	7.5 m/s
δ_0: initial of rudder angle	0 deg	0 deg
$\dot{\delta}_{\max}$: maxi rotation velocity of rudder	2.7 deg/s	2.7 deg/s
n_0: initial shaft velocity	57 rpm	80 rpm
n_c: shaft velocity command	57 rpm	80 rpm
δ_c: rudder command	-35 deg	[-20,+20] deg

Subscripts *cal* and *exp* indicate the computed and experimental data respectively, (x_i, y_i) are the coordinates of the point i on the ship's trajectory, and N_p is the number of pairs of points to be approximated. (ii) For the Zig-Zag test, the expression of $F_{ob\,j}$ reads:

$$F_{obj} = \left(\sum_{i=1}^{N} f_i(\alpha)^2 \right)^{1/2} = \left(\sum_{i=1}^{N} \left(\psi_i^{cal} - \psi_i^{\exp} \right)^2 \right)^{1/2} \tag{16}$$

Where: ψ_i is the ship's heading angle, which depends also on ship hydrodynamic coefficients α; N_p is the number of pairs of points to be approximated.

3.2. Numerical results

The validation of the present investigation is done for the Esso Bernicia 193000DWT Tanker model [10], where the associated parameters are given in Table 3. Here, the 35 hydrodynamic parameters (hydrodynamic coefficients) to be identified are given in Table 4.

The numerical identification procedure starts from original values of all hydrodynamic parameters (α) in the dynamic ship motion equations (Eq. 2-4), which will be firstly analyzed through a sensitivity analysis sensitivity analysis will show how important is the relative gradient value of $F_{ob\,j}$ response for a small variation of the hydrodynamic coefficient α_i.

Table 3: Parameters of the Esso Bernicia 193000DWT Tanker model [10]

Ship parameters	Value
L_{pp}: length between perpendicular	304.8 (m)
B: beam	47.17 (m)
T : draft to design waterline	18.46 (m)
∇: displacement	220000 (m^3)
L_{pp}/B	6.46
B/T	2.56
C_B: block coefficient	0.83
U_0: design speed	16 (knots)
n: nominal propeller	80 (rpm)

By using Eq. 14-16, the most sensitive hydrodynamic coefficients are identified and are summarized in Table 5 and Table 6.

The simulation and optimization procedure consists on the following steps:

• Step 1: Computing and simulation of ship trajectories with original coefficients (α) from dynamic ship motion equations Eq. 1-4.

• Step 2: Filtering the most important coefficients (α_S) among all others (α), based on the sensitivity analysis
• Step 3: Computing of optimal values ($\alpha_{S\ opt}$) for only most sensitive coefficients (α_S), by carrying out an optimization analysis based on a optimization procedure.

Table 4: Original hydrodynamic coefficients of Esso Bernicia 193000DWT Tanker model [10]

No id.	Coefficient	Reference Value
1	$X''_{\dot{u}}$	-0.05
2	X''_{vr}	1.020
3	$Y''_{\dot{v}}$	-0.020
4	$Y''_{\lvert c\rvert c\lvert\beta\rvert\beta\delta}$	-2.16
5	Y''_{T}	0.04
6	N''_{T}	-0.02
7	$N''_{\dot{r}}$	-0.0728
8	$Y''_{\lvert v\rvert v}$	-2.4
9	$N''_{\lvert v\rvert r}$	-0.3
10	$X''_{\lvert v\rvert v}$	0.3
11	Y''_{uv}	-1.205
12	N''_{uv}	-0.451
13	$X''_{\dot{u}\xi}$	-0.05
14	$Y''_{\dot{v}\xi}$	-0.378
15	$Y''_{ur\xi}$	0.182
16	$N''_{ur\xi}$	-0.047
17	$X''_{vr\xi}$	0.378
18	$Y''_{\lvert v\rvert v\xi}$	-1.5
19	$N''_{vr\xi}$	-0.12
20	$Y''_{\lvert c\rvert c\delta}$	0.208
21	$Y''_{uv\xi}$	0
22	$N''_{uv\xi}$	-0.241
23	$X''_{c\lvert c\rvert\beta\delta}$	0.152
24	$N''_{c\lvert c\rvert\delta}$	-0.098
25	$X''_{vv\xi\xi}$	0.0125
26	$Y''_{\lvert c\rvert c\lvert\beta\rvert\beta\delta}$	-2.16
27	$N''_{\lvert c\rvert c\lvert\beta\rvert\beta\delta}$	0.688
28	$Y''_{\lvert c\rvert c\lvert\beta\rvert\beta\delta\xi}$	-0.191
29	$N''_{\lvert c\rvert c\lvert\beta\rvert\beta\lvert\delta\rvert\xi}$	0.344
30	Y''_{ur}	0.248
31	N''_{ur}	-0.207
32	$X''_{\mathrm{u}\lvert\mathrm{u}\rvert}$	-0.0377
33	$N''_{\dot{r}\xi}$	-0.0045
34	$X''_{\lvert\mathrm{u}\rvert\mathrm{u}\xi}$	-0.0061
35	$X''_{c\lvert c\rvert\delta\delta}$	-0.093

Table 5: Most sensitive coefficients of Turning Circle and Zig-Zag tests

No id.	Coefficient
6	N''_{T}
15	$Y''_{ur\xi}$
16	$N''_{\mathrm{ur}\xi}$
22	$N''_{\mathrm{uv}\xi}$
34	$X''_{\lvert u\rvert u\xi}$
24	$N''_{\lvert c\rvert c\delta}$

Table 6: Independent most sensitive coefficients for the Esso Bernicia 193000DWT Tanker model

No id.	Turning circle test	No id.	Zig-zag test
20	$Y''_{\lvert c\rvert c\delta}$	7	$N''_{\dot{\mathrm{r}}}$
23	$X''_{c\lvert c\rvert\beta\delta}$	32	X''_{uu}
31	N''_{ur}	33	$N''_{\dot{\mathrm{r}}\xi}$
35	$X''_{c\lvert c\rvert\delta\delta}$	5	Y''_{T}

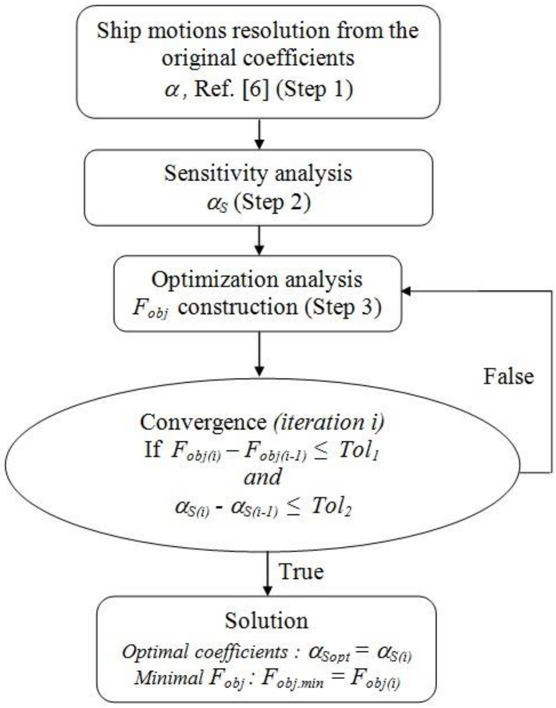

Fig.2: Flowchart of the optimization procedure

The flowchart of the optimization procedure is shown in Fig.2. In the minimization procedure, we deal with disparate values of the objective function F_{obj} . Thus, we have to normalize the objective function by the following scaling:

$$\bar{F}^{iter}_{obj} = \frac{F^{iter}_{obj}}{F^{0}_{obj}} \tag{17}$$

where *iter* is the iteration number and F_{obj}^{0} corresponds to the objective function value in the initial iteration.

3.3. Validation tests

3.3.1. Turning Circle test

The validation process consists on computing the discrepancy between computed and experimental data. Thus, in order to analyze the discrepancy of ship trajectory we used the Root Mean Square Deviation (RMSD) given by:

$$\Delta S_{(RMSD)} = \left(\frac{1}{N} \sum_{i=1}^{N} \Delta S_i^2 \right)^{1/2} \tag{18}$$

Where: ΔS_i^2 is given by Eq. (15); N is the total of points to be optimized.

Validation tests are carried out by using SQP and BFGS algorithms. The optimal hydrodynamic coefficients obtained by SQP and BFGS algorithms are presented in Table 8.

Before optimization, we obtained from Eqs. 15-20:

$\Delta S_{(RMSD)}$ = 68m.

After minimization, the optimal solutions obtained by both SQP and BFGS algorithms are summarized in Table 7.

Table 7: Numerical results of the minimization procedure for Turning Circle test

	SQP	BFGS
error: $\left\| F_{obj}^{iter} - F_{obj}^{iter-1} \right\|$	1 x 10^{-4}	1 x 10^{-4}
error: $\left\| \alpha_S^{iter} - \alpha_S^{iter-1} \right\|$	1 x 10^{-4}	1 x 10^{-4}
Max Nb iterate	29	9
Min F_{obj}	0.084	0.120
$\Delta S_{(RMSD)}$ (m)	5.8	8.0

The optimal ship trajectory is given in Fig.3, and the convergence of objective function is given in Fig.4. Fig.4 shows that by using the same tolerances for the two algorithms, we see that SQP algorithm converged after 30 iterations while BFGS algorithm converges only in 10 iteration.

However, the computing time of SQP algorithm is smaller than that of BFGS algorithm. Otherwise, the variation of the objective function during the iterations of SQP algorithm is more convergent than that of BFGS algorithm. Also, we notice a very good results of RMSD of discrepancy of ship trajectory after minimization, which are 5.8m and 8.0m by using SQP and BFGS algorithms respectively, whereas prior to the minimization the RMSD was 68.0 m (Tab.7). This shows that ΔS (see Eq.15) obtained by SQP algorithm is more satisfactory than that obtained by BFGS algorithm.

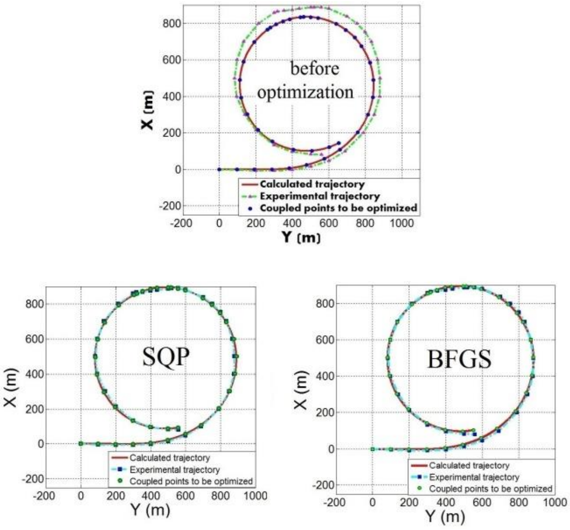

Fig.3: Ship trajectory before and after optimization (Turning Circle test)

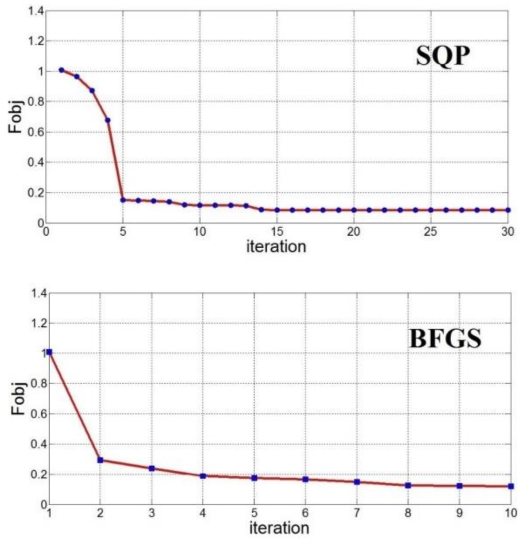

Fig.4: Convergence of the objective function (Turning Circle test)

We note also the remarkable low values of the objective function obtained by SQP and BFGS algorithms after convergence, which are 0.084 and 0.120 respectively. It shows that SQP algorithm is the best optimization algorithm for Turning Circle test.

The surge force, sway force and yaw moment before and after optimization in case of using the SQP method are presented in Fig.5. This shows that at the beginning of Turning Circle test, the absolute value of forces and moment are reduced, thus the Turning radius is reduced also after optimization. We can explain this phenomenon by comparing the value of hydrodynamic coefficients before and after using the SQP method in Tab.8 and Eq. 2-4.

Table 8: Optimal hydrodynamic coefficients in Turning Circle test

Variables	Coefficient	Original value	Optimal value (SQP)	Optimal value (BFGS)
x(1)	$N_T^{''}$	-0.02	**-0.0240**	**-0.0207**
x(2)	$Y_{ur\xi}^{''}$	0.182	**0.1598**	**0.1822**
x(3)	$N_{\mathrm{ur}\xi}^{''}$	-0.047	**-0.0416**	**-0.0533**
x(4)	$Y_{\|c\|c\delta}^{''}$	0.208	**0.1761**	**0.2052**
x(5)	$N_{uv\xi}^{''}$	-0.241	**-0.2823**	**-0.2400**

x(6)	$X''_{c\|c\|\beta\delta}$	0.152	**0.1684**	**0.1519**
x(7)	$N''_{\|c\|c\delta}$	-0.098	**-0.0805**	**-0.0942**
x(8)	N''_{ur}	-0.207	**-0.2105**	**-0.2096**
x(9)	$X''_{\|u\|u\xi}$	-0.0061	**-0.0073**	**-0.0065**
x(10)	$X''_{c\|c\|\delta\delta}$	-0.093	**-0.1000**	**-0.0936**

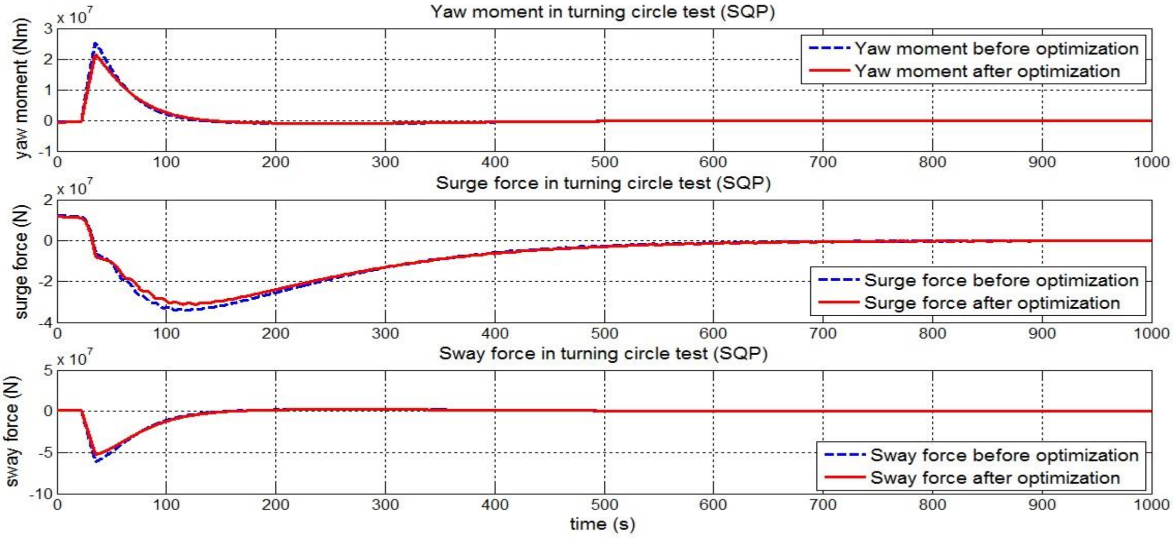

Fig.5: Surge force, sway force and yaw moment (turning Circle test, SQP method)

Firstly, among the components of surge force in Turning Circle test, $X''_{c|c|\delta\delta}c|c|\delta^2$ is the most important component because this is the component that acts on the rudder surface in GX_0 axis when the rudder rotates. $\left|X''_{c|c|\delta\delta}\right|$ increased from -0.093 to -0.1000, which means that the resistance of rudder in GX_0 axis was increased, thus the ship turns more difficultly on to the port side.

Secondly, $Y''_{|c|c\delta}|c|c\delta$ is the most important component that acts on the rudder surface in GY_0 axis. $Y''_{|c|c\delta}$ reduced from 0.208 to 0.1761, which means that the ship turns more slowly on to the port side.

Finally, $N''_{|c|c\delta}|c|c\delta$ is the most important component in yaw moments, which caused by the components of rudder forces when the rudder rotates. $\left|N''_{|c|c\delta}\right|$ reduced from -0.098 to -0.085, which means that yaw moment is reduced when the rudder rotates to the port side.

For conclusion, by applying the SQP algorithm to optimize the ship trajectory in Turning Circle test, the turning radius was increased, which means that the optimal ship trajectory is more close to the experimental trajectory as Fig.3.

3.3.2. Zig-Zag test

By using Eq. 20, we obtained the RMSD of the discrepancy between computed and experimental heading angles of ship before minimization, which is: $\Delta\psi_{(RMSD)}$ = 17.3 deg.

The optimal hydrodynamic coefficients are presented in Tab. 8. Computed and experimental headings of ship before and after minimization are given in Fig. 8. It shows that by using SQP algorithm the computed heading angle can approximate to experimental heading angle after 400 sec., whereas BFGS algorithm does it after 700 sec.

By using the same tolerances of minimization variable for the two algorithms, the SQP algorithm converged after 18 iterations whereas BFGS algorithm converges only after 3 iterations (Fig.7). However, the computed time of the SQP algorithm is smaller than that of BFGS algorithm.

Also, we notice satisfactory results of RMSD of discrepancy of ship's heading angles after minimization, which are 6.6 degs and 7.1 degs by using SQP and BFGS algorithms respectively, while its value before minimization is 17.3 degs (Fig.6). This means that the reduction of discrepancy between computed and experimental heading angle obtained by SQP algorithm is more considerably than that by BFGS algorithm.

We note also the low value of the objective function after convergence are 0.365 and 0.389 by using SQP and BFGS algorithms respectively. It means that the final value of objective function by using the SQP algorithm is smaller than that by using BFGS algorithm. Finally, for these reasons we conclude that the SQP algorithm is the best optimization algorithm for Zig-Zag test.

Fig.8 shows surge force, sway force and yaw moment before and after optimization by using SQP method.

Table 9: Numerical information of the minimization procedure in Zig-Zag test

	SQP	BFGS
error: $\left\|F_{obj}^{iter} - F_{obj}^{iter-1}\right\|$	1 x 10^{-4}	1 x 10^{-4}
error: $\left\|\alpha_S^{iter} - \alpha_S^{iter-1}\right\|$	1 x 10^{-4}	1 x 10^{-4}
Max Nb iterate	18	3
Min F_{obj}	0.365	0.389
$\Delta S_{(RMSD)}$ (m)	6.6	7.1

3.4. Identification of hydrodynamic parameters

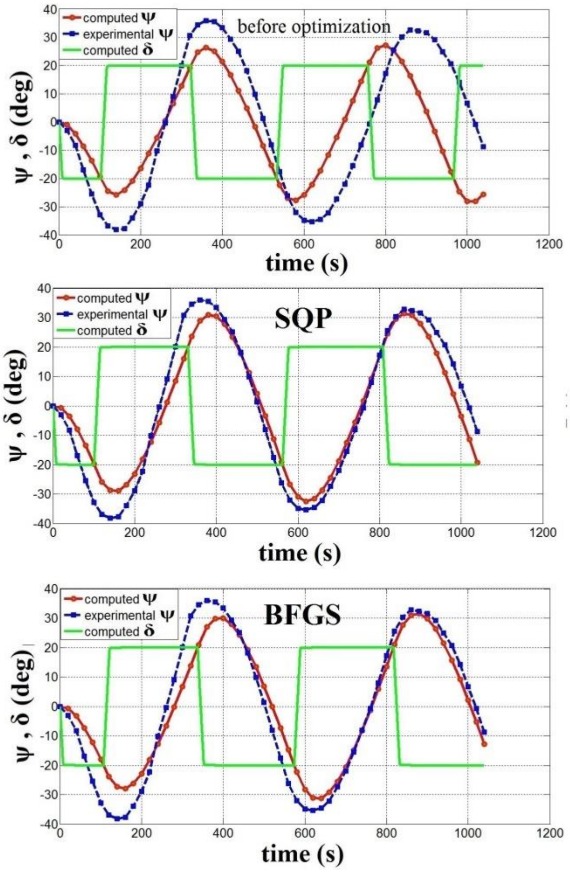

Fig.6: Heading angle (yaw angle) of ship before and after minimization (Zig-Zag test). comparison between computed results and experimental data.

From the result of coefficient identification for Turning Circle and Zig-Zag tests (Section 3.3), we can choose finally a set of identified hydrodynamic coefficients for Esso Bernicia 193000DWT Tanker model, which may be used both for these two tests and other maneuvering simulations. This set has 35 hydrodynamic coefficients, which includes the average optimal values of 6 common most sensitive coefficients, the optimal values of 8 independent most sensitive coefficients of each test, and 21 other original coefficients that influence weakly the gradient of objective function. For more details, we summarize all of coefficients before and after identification in Table 11-12.

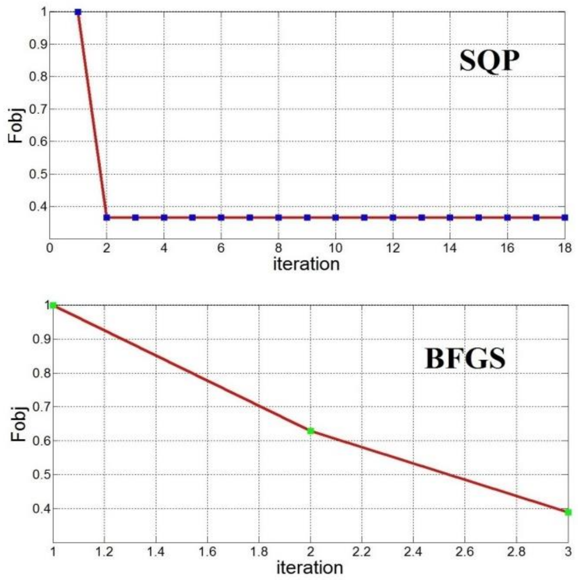

Fig.7: Converge of objective function (Zig-Zag test)

Table 10: Optimal hydrodynamic parameters in Zig-Zag test

Variables	Coefficient	Original value	Optimal value (SQP)	Optimal value (BFGS)
x(1)	Y''_T	0.04	0.0300	0.0356
x(2)	N''_T	-0.02	-0.0160	-0.0006
x(3)	$N''_{\dot{r}}$	-0.0728	-0.0878	-0.0813
x(4)	$Y''_{ur\xi}$	0.182	0.1420	0.1783
x(5)	$N''_{ur\xi}$	-0.047	-0.0380	-0.0383
x(6)	$N''_{uv\xi}$	-0.241	-0.2910	-0.2434
x(7)	$N''_{\|c\|c\delta}$	-0.098	-0.0800	-0.0941
x(8)	X''_{uu}	-0.0377	-0.0457	-0.0395
x(9)	$N''_{\dot{r}\xi}$	-0.0045	-0.0054	-0.0254
x(10)	$X''_{\|u\|u\xi}$	-0.0061	-0.0073	-0.0104

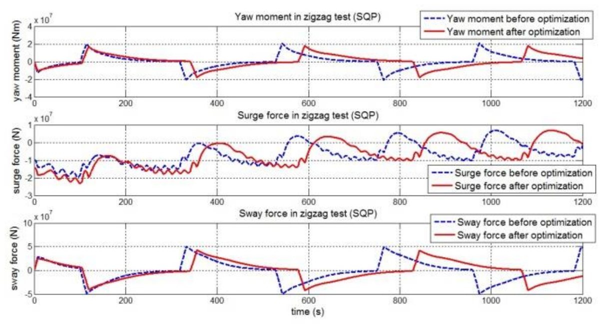

Fig.8: Surge force, sway force and yaw moment (Zig-Zag test, SQP algorithm)

Table 11: Identified hydrodynamic coefficients for the Esso Bernicia 193000DWT Tanker model
(First part of the list).

No id.	Hydrody-namic coefficients	Original values	Optimal values (Turning test)	Optimal values (Zig-Zag test)	Identified values
1	$X''_{\dot{u}}$	-0.0500	-	-	**-0.050**

2	X''_{vr}	1.0200	-	-	**1.0200**
3	$Y''_{\dot{v}}$	-0.0200	-	-	**-0.020**
4	$Y''_{\|c\|c\|\beta\|\beta\delta}$	-2.16	-	-	**-2.16**
5	Y''_{T}	0.0400	-	0.0300	**0.030**
6	N''_{T}	-0.0200	-0.0240	-0.0160	**-0.020**
7	$N''_{\dot{r}}$	-0.0728	-	-0.0878	**-0.087**
8	$Y''_{\|v\|v}$	-2.4000	-	-	**-2.400**
9	$N''_{\|v\|r}$	-0.3000	-	-	**-0.300**
10	$X''_{\|v\|v}$	0.3000	-	-	**-1.2050**
11	Y''_{uv}	-1.2050	-	-	**-0.4510**
12	N''_{uv}	-0.4510	-	-	**-0.0500**
13	$X''_{\dot{u}\xi}$	-0.0500	-	-	**-0.3780**
14	$Y''_{\dot{v}\xi}$	-0.3780	-	-	**0.1509**
15	$Y''_{ur\xi}$	0.1820	0.1598	0.1420	**-0.04**
16	$N''_{ur\xi}$	-0.0470	-0.0416	-0.0380	**0.0378**
17	$X''_{vr\xi}$	0.3780	-	-	**-1.500**
18	$Y''_{\|v\|v\xi}$	-1.5000	-	-	

Table 12: Identified hydrodynamic coefficients for the Esso Bernicia 193000DWT Tanker model
(Second part of the list).

No id.	Hydrodynam-ic coefficients	Original values	Optimal values (turning test)	Optimal values (zig-zag test)	Identified values
19	$N''_{vr\xi}$	-0.1200	-	-	**-0.120**
20	$Y''_{\|c\|c\delta}$	0.2080	0.1761	-	**0.1761**
21	$Y''_{uv\xi}$	0.0000	-	-	**0.0000**
22	$N''_{uv\xi}$	-0.2410	-0.2823	-0.2910	**-0.287**
23	$X''_{c\|c\|\beta\delta}$	0.1520	0.1684	-	**0.1684**
24	$N''_{\|c\|c\delta}$	-0.0980	-0.0805	-0.0800	**-0.080**
25	$X''_{vv\xi\xi}$	0.0125	-	-	**0.0125**
26	$Y''_{\|c\|c\|\beta\|\beta\delta}$	-2.1600	-	-	**-2.160**
27	$N''_{\|c\|c\|\beta\|\beta\delta}$	0.6880	-	-	**0.6880**
28	$Y''_{\|c\|c\|\beta\|\beta\delta\xi}$	-0.1910	-	-	**-0.191**
29	$N''_{\|c\|c\|\beta\|\beta\delta\xi}$	0.3440	-	-	**0.3440**
30	Y''_{ur}	0.2480	-	-	**0.2480**
31	N''_{ur}	-0.2070	-0.2105	-	**-0.210**
32	$X''_{u\|u\|}$	-0.0377	-	-0.0457	**-0.046**
33	$N''_{\dot{r}\xi}$	-0.0045	-	-0.0054	**-0.005**
34	$X''_{\|u\|u\xi}$	-0.0061	-0.0073	-0.0073	**-0.007**
35	$X''_{c\|c\|\delta\delta}$	-0.0930	-0.1000	-	**-0.100**

4. Conclusion

A ship manoeuvring numerical procedure based on the coupling between ship dynamic motion model and optimization techniques is presented. Numerical identification of hydrodynamic parameters is carried out by considering a constrained minimization problem based on the SQP algorithm, and an unconstrained minimization problem based on the BFGS algorithm.
The model was validated using experimental data of sea trials of Esso Bernicia 193000DWT Tanker for the Turning Circle and Zig-Zag tests. The identification procedure was carried out successfully for the 14 most sensitive hydrodynamic parameters, after a preliminary screening using sensitivity analysis.
In the Turning Circle test, we found that the SQP algorithm predicted accurately the experimental trajectories, with a RMSD of 5.8m, starting from an initial value of 69m (before optimization), which means that this RMSD was decreased by 91.6%.
In the Zig-Zag test of ship heading, the SQP algorithm gave a RMSD of 6.6 deg, starting from an initial value of 17.3 deg (before optimization), which means that this RMSD was decreased by 61.8%.
Finally, we choose and proposed a set of identified hydrodynamic parameters for Esso Bernicia 193000DWT Tanker model, which may be used for both the Turning circle, Zig-Zag tests and other maneuvering simulations.

5. Acknowledgment

The authors are gratefully to the Vietnam Maritime University (VIMARU) for providing necessary research facilities during current research work.

References

[1] Neves M.A.S., Rodriguez C.A., *A coupled non-linear mathematical model of parametric resonance of ships in head seas*, Applied Mathematical Modelling 33, pp. 2630-2645 (2009)
[2] Sutulo S., Moreira L., Soares C.G., *Mathematical models for ship path prediction in manoeuvring simulation systems*, Ocean Engineering 29, pp. 1-19 (2002)
[3] Yoshimura Y., *Mathematical Model for Manoeuvring Ship Motion*, Workshop on Mathematical Models for Operations in-volving Ship-Ship Interaction, Tokyo 2005 (2005)
[4] Yoon H.K. and Rhee K.P., *Identification of hydrodynamic coefficients in ship manoeuvring equations of motion by Estimation-Before-Modeling technique*, Ocean Engineering 30, pp. 2379-2404 (2003)
[5] Viviani M., Bonvino C.P., Depascale R., Conti F. and Soave M., *Identification of Hydrodynamic Coefficients from Standard Manoeuvres for a Series of Twin-Screw Ships*, 2nd International Conference on Marine Research and Transportation (ICMRT'07), Italia, pp. 99-108 (2007)
[6] Rajesh G. and Bhattacharyya S.K., *System identification for nonlinear manoeuvring of large tankers using artificial neural network*, Applied Ocean Research 30, pp. 256-263 (2008)
[7] Obreja D., Nabergoj R., Crudu L., Pacuraru-Popoiu S., *Identification of hydrodynamic coefficients for manoeuvring simulation model of a fishing vessel*, Ocean Engineering 37, pp. 678-687 (2010)
[8] Zhang X.G. and Zou Z.J., *Identification of Abkowitz model for ship manoeuvring motion using E-support vector regression*, Journal of Hydrodynamics, pp. 353-360 (2011)
[9] Seo M.G. and Kim Y., *Numerical analysis on ship maneuvering coupled with ship motion in waves*, Ocean Engineering, Vol.38, N17-18, pp.1934 - 1945 (2011)

[10] Fossen T.I., *Guidance and Control of Ocean Vehicles*, John Wiley&Sons, 448 pages (1994)
[11] Antoniou A. and Lu W.S., *Practical Optimization: Algorithms and Enginnering Applications*, Springer, 202 pages (2007)
[12] Zhang J. and Zhang X., *A robust SQP method for optimization with inequality constraints*, *Journal of Computational Mathematics*, Vol. 21, No. 2, pp. 247-256 (2003)
[13] Dai Y.H., *Convergence properties of the BFGS algorithm,* Society for Industrial and Applied Mathematics, SIAM J.OPTIM, Vol. 13, No. 3, pp. 693-701 (2002)
[14] Bertram V., *Pratical Ship Hydrodynamics*, Butterworth-Heinemann, 270 pages (2000)
[15] Lopez E., Velasco F.J., Moyano E. and Rueda T.M., *Full-sacale maneuvering trials simulation*, Journal of Maritime Research-JMR, Vol.I, No. 3, pp.37-50 (2004)
[16] Clarke, D.; Patterson, D.R.; Vfooderson, R.K., *Manoeuvring trials with the 193,000 tonne deadweight tanker "Esso Bernicia".,* Paper: Spring Meeting of the Royal Inst, of Naval Architects, No. 10, 14 (1972)
[17] Kreuzer E., Pick M.A., *Dynamics of Ship Motion*, PAMM Proc. Appl. Math. Mech. 3, 84-87 (2003) / DO 10.1002/pamm.20031032